Supporting Information

Sugita et al. 10.1073/pnas.1015819107

SI Materials and Methods

Computational details. All-atom MD simulations of sarcoplasmic reticulum (SR) Ca^{2+}-ATPase with bound Ca^{2+}, explicit solvent, and phospholipids were carried out using MARBLE software package (1). CHARMM27 force field parameters for proteins (2), phospholipids, and ions, except for Ca^{2+} were used. TIP3P model (3) was used for water molecules. The Lennard–Jones parameters for Ca^{2+} were taken from the ion parameters developed by Åqvist (4), because the hydration free energies for a series of divalent cations have been reproduced with the parameter sets. Periodic boundary conditions with no truncation using the particle mesh Ewald (PME) algorithm were employed (5, 6). The Lennard–Jones interactions were switched to zero over a range of 8–10 Å using an atom-based cut-off. All water molecules and all CHx, NHx, ($x = 1,2,3$), SH, and OH groups in the protein and lipids were treated as rigid-bodies (1). The equation of motion was integrated with a time step of 2 fs. In the MD simulations, pressure and temperature of the simulation system were controlled to 1 atm and 300 K by using the constant area-isothermal isobaric (NPAT) algorithm (7).

The starting structures for wild-type Ca^{2+}-ATPase bound with two Ca^{2+} were taken from a crystal structure of the enzyme [Protein Data Bank (PDB) ID: 1su4] (8). Glu58 and Glu908 were treated as protonated (9). The starting structures for Glu771Gln or Glu908Gln were made by substituting the Glu in the wild-type structure with Gln keeping the side chain conformation unchanged. In Glu771Gln, the ionization states of the glutamates were the same as those in wild-type; only Glu58 was treated as protonated in Glu908Gln. Detailed procedures for setting up a full simulation system including a Ca^{2+}-ATPase, 473 dioleoylphosphatidylcholine phospholipids, two bound Ca^{2+}, 150 mM salt solution were described previously (9). After 1-ns equilibration, we performed three 10-ns molecular dynamics (MD) simulations for wild-type (WT1, WT2, and WT3), Glu771Gln (E771Q1, E771Q2, and E771Q3), and Glu908Gln (E908Q1, E908Q2, and E908Q3). All the coordinates of the simulation system were saved every 1 ps during production dynamics. For structural comparison, Cα atoms of the residues on the M7–M10 helices were fitted to those in the crystal structure.

1. Ikeguchi M (2004) Partial rigid-body dynamics in NPT, NPAT, and NPγT ensembles for proteins and membranes. *J Comput Chem* 25:529–541.
2. Mackerell AD, et al. (1998) All-atom empirical potential for molecular modeling and dynamics studies of proteins. *J Phys Chem B* 102:3586–3616.
3. Jorgensen WL, Chandrasekhara J, Madura JD, Impey RW, Klein ML (1983) Comparison of simple potential functions for simulating liquid water. *J Chem Phys* 79:926–935.
4. Åqvist J (1990) Ion–water interaction potentials derived from free-energy perturbation simulations. *J Phys Chem* 94:8021–8024.
5. Darden T, York D, Pedersen L (1993) Particle mesh Ewald: An N ⊕ log(N) method for Ewald sums in large systems. *J Chem Phys* 98:10089–10092.
6. Essmann U, et al. (1995) A smooth particle mesh ewald method. *J Chem Phys* 103:8577–8593.
7. Zhang Y, Feller SE, Brooks B, Pastor RW (1995) Computer simulation of liquid/liquid interfaces, I. Theory and application to octane/water. *J Chem Phys* 103:10252–10266.
8. Toyoshima C, Nakasako M, Nomura H, Ogawa H (2000) Crystal structure of the calcium pump of sarcoplasmic reticulum at 2.6 Å resolution. *Nature* 405:647–655.
9. Sugita Y, Miyashita N, Ikeguchi M, Kidera A, Toyoshima C (2005) Protonation of the acidic residues in the transmembrane cation-binding sites of the Ca^{2+} pump. *J Am Chem Soc* 127:6150–6151.

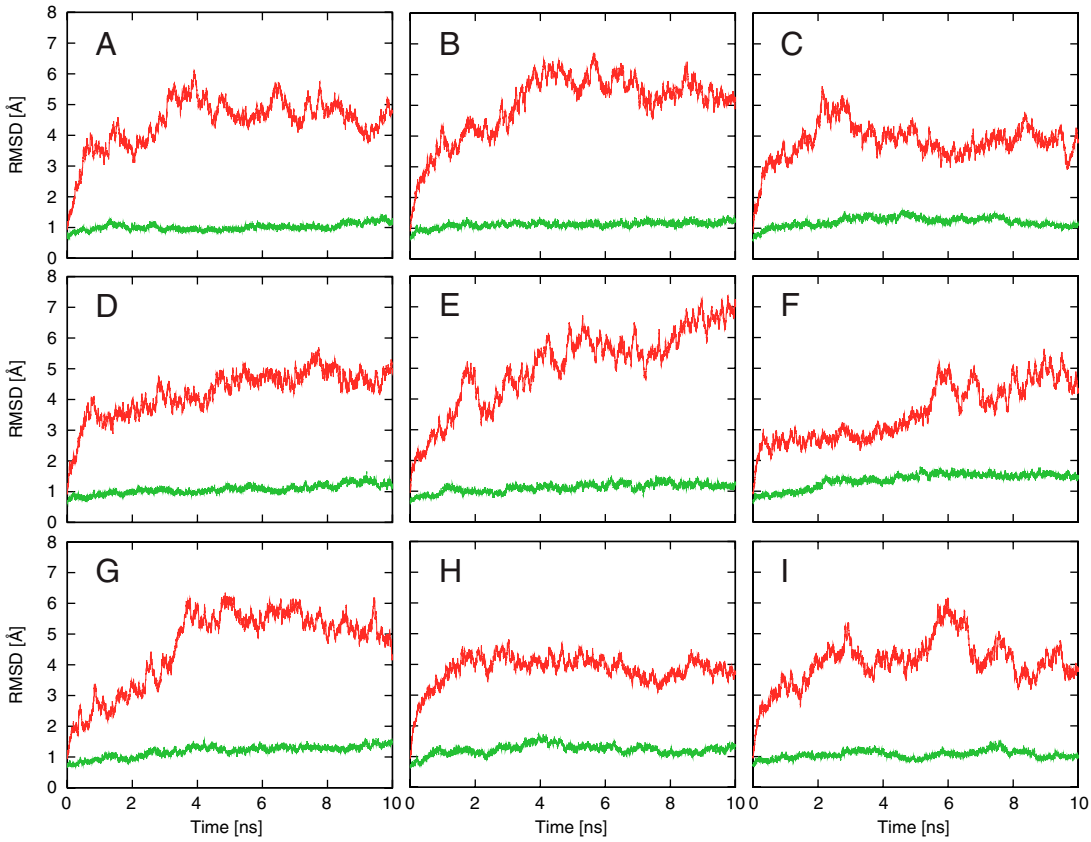

Fig. S1. The root mean square deviations (RMSD) of Cα atoms from the crystal structure (PDB ID: 1SU4). The RMSD for the simulations of wild-type [(*A*) WT1, (*B*) WT2, and (*C*) WT3], for those of the Glu771Gln mutant [(*D*) E771Q1, (*E*) E771Q2, and (*F*) E771Q3], and for those of the Glu908Gln mutant [(*G*) E908Q1, (*H*) E908Q2, and (*I*) E908Q3]. Red and green lines represent the RMSD calculated for a full structure and the transmembrane helices of the Ca^{2+}-ATPase, respectively.

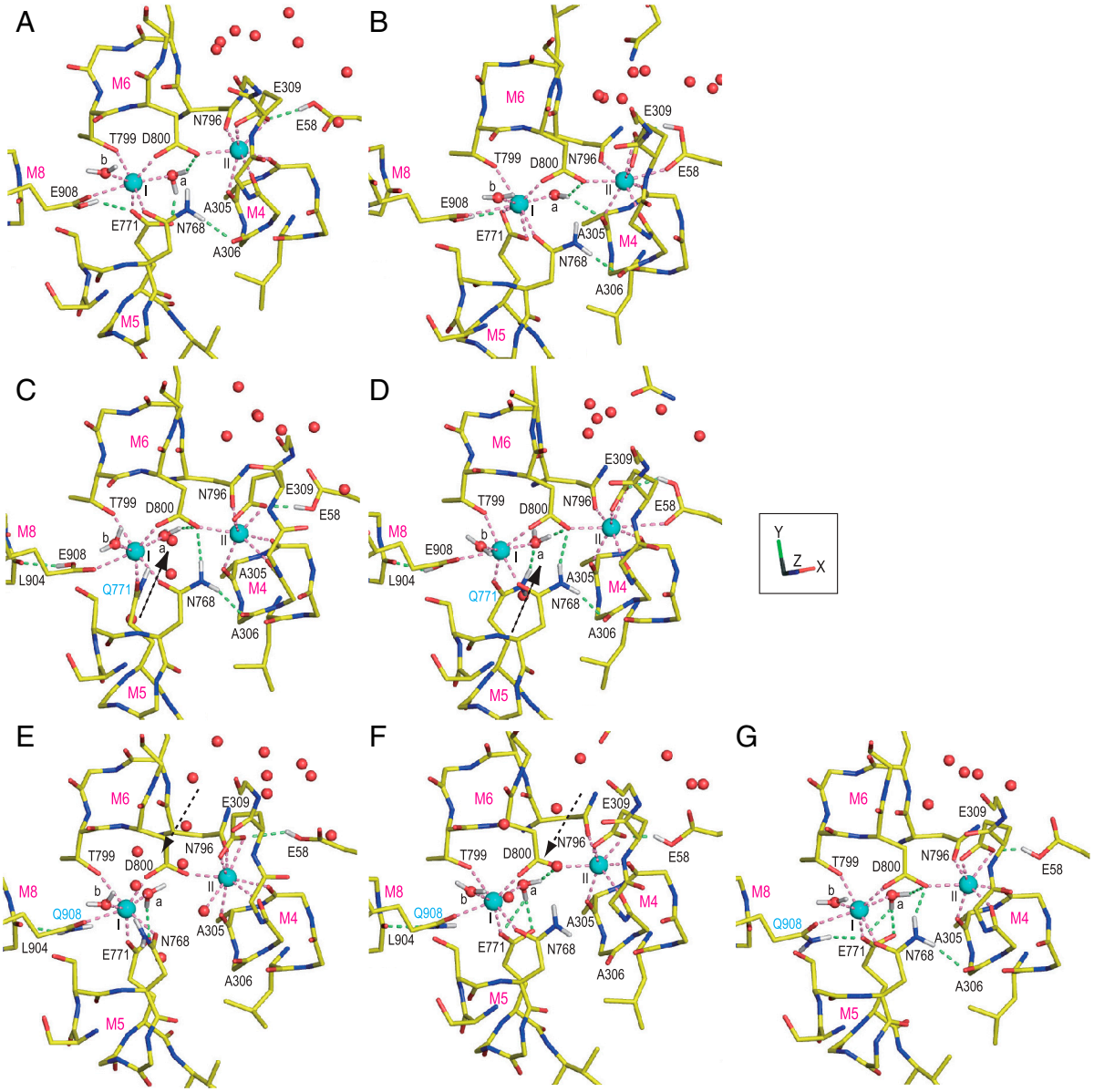

Fig. S2. Snapshots of the Ca^{2+}-bindig sites in MD simulations. At 10 ns of the simulations for wild-type [(*A*) WT2 and (*B*) WT3], Glu771Gln [(*C*) E771Q1, and (*D*) E771Q2], and Glu908Gln mutant [(*E*) E908Q1, (*F*) E908Q2, and (*G*) E908Q3)] viewed from the cytoplasm. Presented in the same way as in Figs. 2 and 4. The dashed arrows in *C* and *D* represent flows of water molecules from the lumen, whereas the dashed arrows in Fig. S2 *E* and *F* represent invasion of water molecules from the cytoplasm.

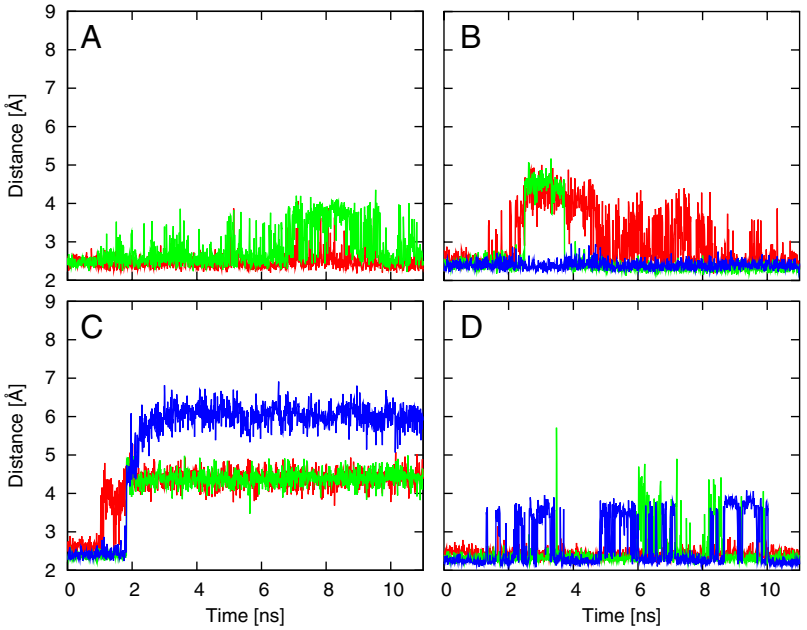

Fig. S3. Time-series of the Ca^{2+}-binding distances. (*A*) The distances between site II Ca^{2+} and the Ala305 carbonyl (red), and between site I Ca^{2+} and the Glu908 carboxyl (green) in a simulation for wild-type (WT1). (*B*) Those between site II Ca^{2+} and the Ala305 carbonyl (red), between site I Ca^{2+} and the Gln771 carbonyl (green), and between the site I Ca^{2+} and Glu908 (blue) in a simulation for the Glu771Gln mutant (E771Q1). (*C*) Those between site II Ca^{2+} and the Ala305 carbonyl (red), between site I Ca^{2+} and the Thr799 hydroxyl (green), between site I Ca^{2+} and the Glu908 carboxyl (blue) in a simulation for the Glu771Gln mutant (E771Q3). (*D*) Those between the site II Ca^{2+} and the Ala305 carbonyl (red), between site I Ca^{2+} and the Asn768 carbonyl (green), between the site I Ca^{2+} and Glu771 carboxyl (blue) in a simulation for the Glu908Gln mutant (E908Q1).

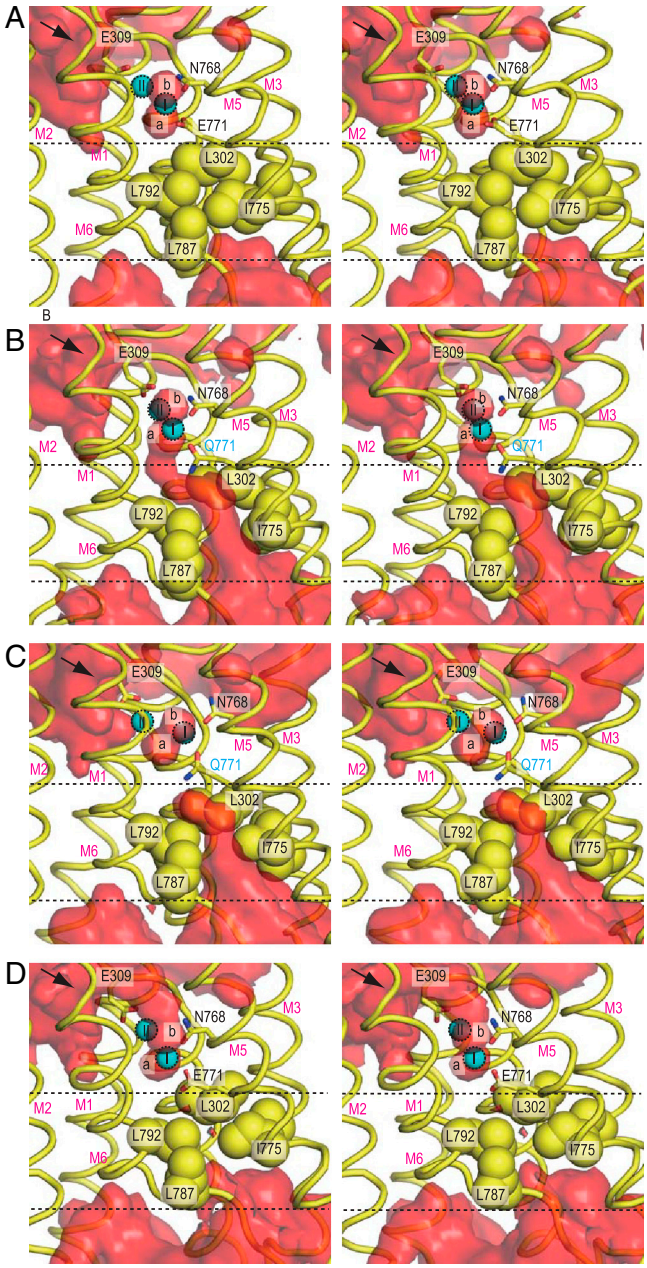

Fig. S4. Stereo views of hydrophobic shielding on the lumenal side. Atomic models obtained in simulations for wild-type [(*A*) WT1 at 10 ns], Glu771Gln [(*B*) E771Q1 at 10 ns and (*C*) E771Q3 at 10 ns], and Glu908Gln mutant [(*D*) E908Q1 at 10 ns]. Presented in the same way as in Fig. 3 in the main text.

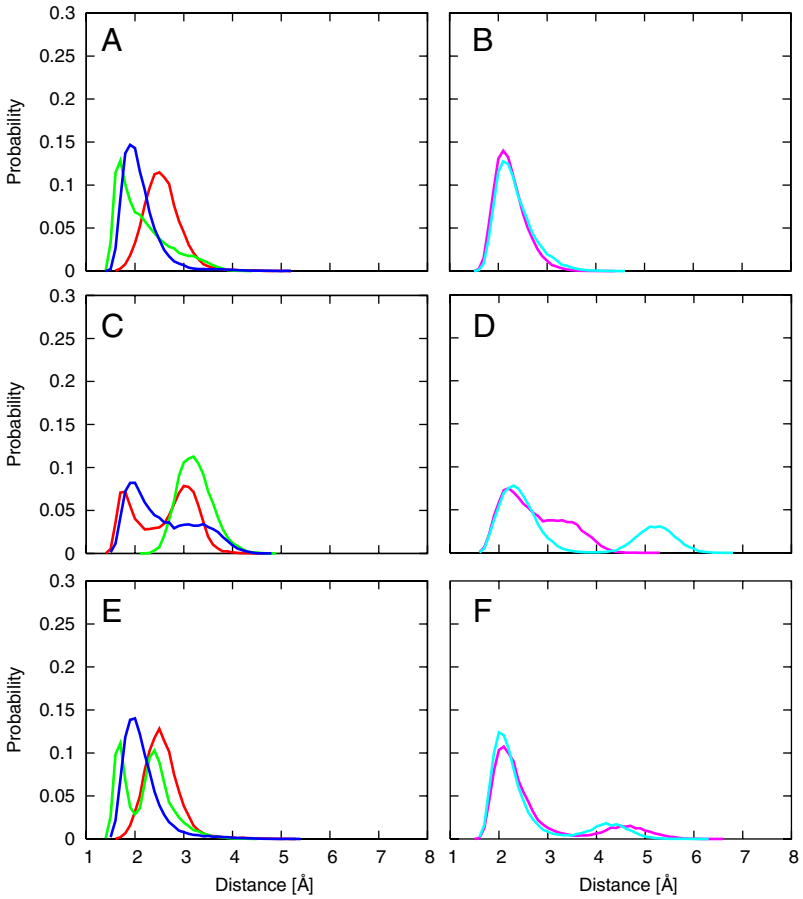

Fig. S5. Distance distributions in simulations between atoms implicated in hydrogen bonds around the bound Ca^{2+}. The distributions calculated from the three simulation trajectories for wild-type (*A* and *B*), Glu771Gln (*C* and *D*), and Glu908Gln (*E* and *F*). In the three left panels (*A*, *C*, and *E*), lines represent the distances between the Ala305 carbonyl oxygen and one of the hydrogen atoms in water **a** (red), those between the Glu771 carboxyl oxygen (or the Gln771 amide nitrogen) and a hydrogen atom in water **a** (green), and those between the Asp800 carboxyl oxygen and a hydrogen atom in water **a** (blue). In the right panels (*B*, *D*, and *F*), lines represent distances between the Ala306 carbonyl oxygen and the Asn768 amide hydrogen (magenta) and those between the Asp800 carboxyl oxygen and the Asn768 amide hydrogen (light blue). We selected the hydrogen atoms in Asn768 and water **a**, which form hydrogen bonds in Fig. 2 in the main text.

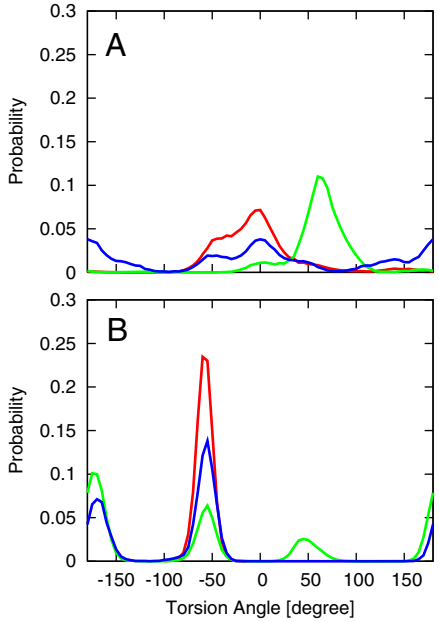

Fig. S6. Distributions of the side chain torsion angles χ_3 in Glu771(Gln771) (*A*) and χ_1 in Ile775 (*B*). In each figure, red, green, blue lines represent the distributions calculated from the three simulation trajectories for wild-type, Glu771Gln, and Glu908Gln mutants, respectively.

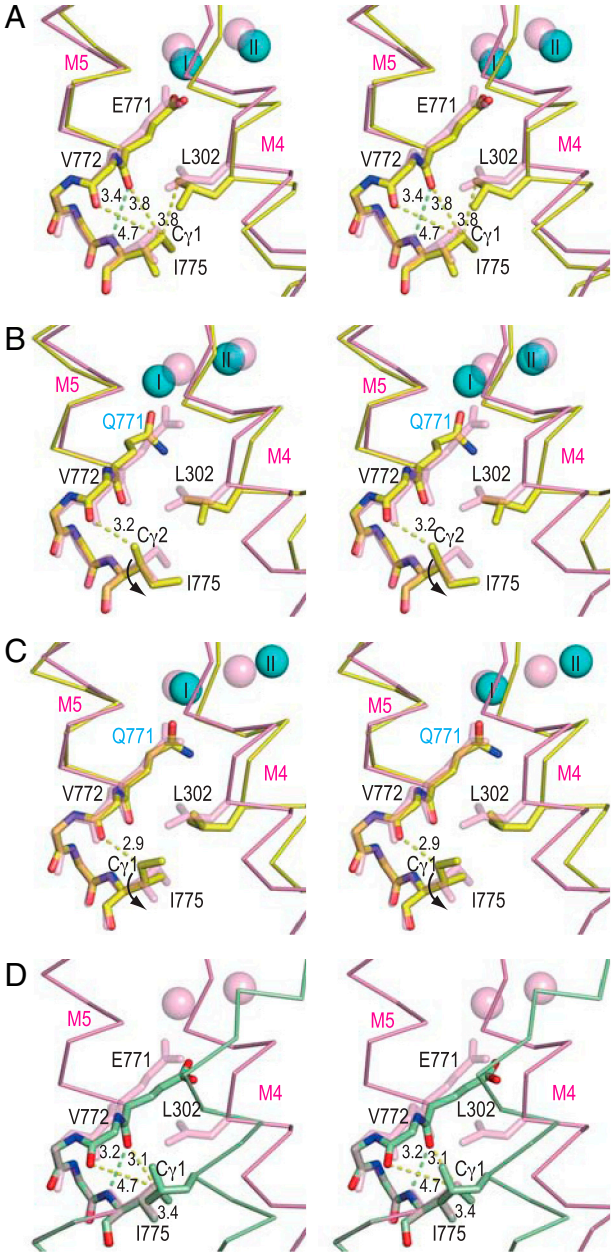

Fig. S7. Close-up stereo views of the transmembrane Ca^{2+}-binding sites in a direction along the membrane plane. The backbone atoms in residues 773–776 were used for superimposing the atomic models in simulations [(*A*) WT1 at 10 ns, (*B*) E771Q1 at 10 ns, (*C*) E771Q3 at 10 ns] and the E2 crystal structure (*D*) with that in the E1·2Ca^{2+} crystal structure (*A–D*; pink). The green and yellow dashed lines show the distances between the Glu771 carbonyl and the Ile775 amide and the nearest distance between the Val772 carbonyl and the Cγ1 or Cγ2 in Ile775. In the E1·2Ca^{2+} crystal structure, the distances between the Val772 carbonyl and the Ile775 side chain would become 2.65 Å and 2.50 Å, if Ile775 took the side chain conformation shown in *B* and *C*, respectively. Corresponding values in the simulations are indicated in *B* and *C*. The arrows in Figs. S7 *B* and *C* show rotations of the Ile775 side chain.

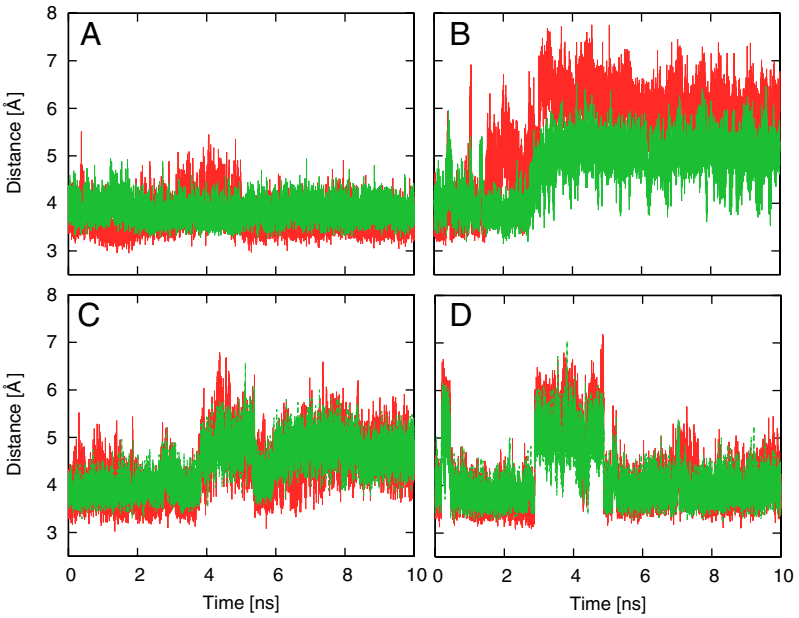

Fig. S8. Time-series of distances from the Ile775 side chain to Glu771 and Leu302. The distances are defined from the Ile775 Cγ1 to the Glu771 carbonyl oxygen (red), and the Leu302 Cδ (green). (*A*) A simulation for wild-type (WT1), (*B*) a simulation for the Glu771Gln mutant (E771Q1), (*C*) a simulation for the Glu771Gln mutant (E771Q3), and (*D*) a simulation for the Glu908Gln mutant (E908Q1).